Molecular Pharmacology Fast Forward. Published on May 24, 2021 as DOI: 10.1124/molpharm.121.000254
This article has not been copyedited and formatted. The final version may differ from this version.

TP53 null mutations identify lung cancer cell lines with highest sensitivity to the non-taxane microtubule inhibitor, eribulin

Trista K. Hinz[1] , Roshni Kalkur[1], Jonathan Rabinovitch[1], Wyatt Hinkle[1] and Lynn E. Heasley[1,2*]

[1]Department of Craniofacial Biology, University of Colorado Anschutz Medical Campus, Aurora, Colorado 80045

and

[2]Eastern Colorado VA Healthcare System, Rocky Mountain Regional VA Medical Center, Aurora, Colorado, USA

Molecular Pharmacology Fast Forward. Published on May 24, 2021 as DOI: 10.1124/molpharm.121.000254
This article has not been copyedited and formatted. The final version may differ from this version.

Running Title: TP53-null lung cancers exhibit high eribulin sensitivity

***Corresponding Author:** Lynn E. Heasley, Department of Craniofacial Biology, School of Dental Medicine, University of Colorado Anschutz Medical Campus, 12801 E. 17th Ave, Aurora, CO 80045, lynn.heasley@cuanschutz.edu

Text pages: 16

Figures: 6

Tables: 2

References: 27

Abstract: 248 words

Introduction: 661 words

Discussion: 1084 words

Non-standard abbreviations: Non-small cell lung cancer, NSCLC; lung adenocarcinoma, LUAD; lung squamous cell carcinoma, LUSC; large cell carcinoma, LCC; small-cell lung cancer, SCLC; epidermal growth factor receptor, EGFR; tyrosine kinase inhibitor, TKI; receptor tyrosine kinase, RTK; Cancer Cell Line Encyclopedia, CCLE;

Molecular Pharmacology Fast Forward. Published on May 24, 2021 as DOI: 10.1124/molpharm.121.000254
This article has not been copyedited and formatted. The final version may differ from this version.

ABSTRACT

The non-taxane microtubule inhibitor, eribulin, is an approved therapeutic for metastatic breast cancer and liposarcoma. Eribulin was previously tested in unselected lung cancer patients and yielded a modest objective response rate of ~5-12 percent. Because lung cancers represent diverse histologies and driving oncogenic mutations, we postulated that eribulin may exhibit properties of a precision oncology agent with a previously undefined specificity for a molecularly distinct subset of lung cancers. Herein, we screened a panel of 44 non-small cell and small cell lung cancer cell lines for in vitro growth sensitivity to eribulin. The results revealed a greater than 15,000-fold range in eribulin sensitivity (IC_{50} = 0.005 – 89 nM) amongst the cell lines that was not correlated with their sensitivity to the taxane-based inhibitor, paclitaxel. The quartile of cell lines exhibiting the lowest eribulin IC_{50} values was not enriched for specific histologies, epithelial-mesenchymal differentiation or specific oncogene drivers, but was significantly enriched for nonsense/frameshift TP53 mutations and low TP53 mRNA, but not missense TP53 mutations. By comparison, the mutation status of CDKN2A, STK11 and KEAP1 were not associated with eribulin sensitivity. Finally, the highest eribulin IC_{50} quartile (>~1 nM) exhibited significantly elevated mRNA expression of the drug pump, ABCB1, a defined resistance mechanism to eribulin and paclitaxel. The findings support further investigations into basic mechanisms by which complete lack of TP53 function regulates anti-cancer activity of eribulin and the potential utility of TP53 null phenotypes distinct from TP53 missense mutations as a biomarker of response in lung cancer patients.

Molecular Pharmacology Fast Forward. Published on May 24, 2021 as DOI: 10.1124/molpharm.121.000254
This article has not been copyedited and formatted. The final version may differ from this version.

SIGNIFICANCE STATEMENT

Distinct from precision oncology agents that are matched to cancers bearing oncogenically-activated versions of their targets, microtubule inhibitors such as eribulin are deployed in an unselected manner. The results in this study demonstrate that lung cancer cell lines exhibiting the highest sensitivity to eribulin bear TP53 null phenotypes, supporting a rationale to consider the status of this tumor suppressor in the clinical setting.

Molecular Pharmacology Fast Forward. Published on May 24, 2021 as DOI: 10.1124/molpharm.121.000254
This article has not been copyedited and formatted. The final version may differ from this version.

INTRODUCTION

Lung cancers have been historically classified by histology where lung adenocarcinoma (LUAD), squamous cell carcinoma (LUSC), large cell carcinoma (LCC) and small cell lung carcinomas (SCLC) represent major subsets. In LUAD, diverse mutationally-activated receptor tyrosine kinases (RTKs) and KRAS serve as oncogene drivers that, when matched with specific small molecule inhibitors, permit implementation of precision oncology for these lung cancers (Camidge et al., 2019; Politi and Herbst, 2015). Moreover, antibody-based inhibitors of the PD1/PD-L1 immunosuppressive axis are now approved for treatment of lung cancers positive for PD-L1 independent of histology (Camidge et al., 2019; Pacheco et al., 2019). Despite this major shift to treatment with molecularly-targeted drugs and immunotherapy, standard chemotherapy continues to serve an important role in the management of lung cancer. Within the class of drugs considered as chemotherapies, microtubule-targeted drugs including the taxanes, vinca alkaloids and eribulin, the focus of this study (Hardin et al., 2017; Swami et al., 2017) represent established and successful therapeutics. Relative to taxanes such as paclitaxel and docetaxel which function as microtubule-stabilizing agents, eribulin, a synthetic derivative of the natural product halichondrin B, inhibits microtubule polymerization resulting in cytosolic accumulation of nonfunctional tubulin aggregates (Hardin et al., 2017; Swami et al., 2017). Eribulin is an approved therapeutic for previously treated metastatic breast cancer and liposarcoma (Swami et al., 2017). In addition, eribulin has been tested in unselected, pretreated lung cancer patients with an objective response rate of 5-12% (Gitlitz et al., 2012; Katakami et al., 2017; Spira et al., 2012; Swami et al., 2017). The phenotypes and genotypes that may associate with eribulin responsiveness in lung cancer patients are not known and represents an important basic research question that could significantly enhance its clinical utility.

As previously noted, precision oncology has greatly changed the therapeutic approach to lung adenocarcinomas (Camidge et al., 2019; Politi and Herbst, 2015). The present approach for treating lung adenocarcinomas bearing oncogenically-mutated epidermal growth factor

Molecular Pharmacology Fast Forward. Published on May 24, 2021 as DOI: 10.1124/molpharm.121.000254
This article has not been copyedited and formatted. The final version may differ from this version.

receptor (EGFR) with targeted tyrosine kinase inhibitors (TKIs) emerged only after initial approval of the EGFR-specific TKI, erlotinib, in unselected patients (Shepherd et al., 2005). Notably, the response rate in the erlotinib-treated group was only 9%, similar to the objective response rate observed with eribulin. In a similarly designed trial, the EGFR-specific TKI, gefitinib, failed to achieve a statistically-significant improvement in overall survival relative to standard chemotherapy despite a similar objective response rate of 8% (Thatcher et al., 2005). It was only after several years of retrospective analysis that a subset of lung cancer patients bearing oncogenic EGFR mutations was mechanistically linked with the observed therapeutic benefit. Moreover, gefitinib was demonstrated in a later phase III trial to provide superior responses in lung cancer patients pre-selected for oncogenic EGFR mutation positivity, but was inferior to standard chemotherapy in EGFR mutation-negative tumors (Mok et al., 2009). Based on these lessons from the clinical development of EGFR-directed TKIs, subsequent targeted agents specific for rearranged, oncogenic forms of ALK and ROS1 were briskly developed in molecularly defined subgroups based on preclinical data prior to clinical testing (Camidge et al., 2019; Politi and Herbst, 2015).

In light of the rather modest response rates of targeted EGFR inhibitors in unselected lung cancer patients, one might consider whether the modest response rates observed for eribulin in unselected, pretreated lung cancer patients may also reflect therapeutic efficacy in a distinct molecular subset of tumors. In the present study, the hypothesis that eribulin exhibits properties of a precision oncology agent with a previously undefined specificity for a molecularly distinct subset of lung cancers was tested. The results reveal that lung cancer cell lines bearing a TP53 null phenotype characterized by nonsense and frameshift mutations or low TP53 mRNA, but not wild-type TP53 or missense TP53 mutations, are enriched in the subset exhibiting the highest sensitivity to eribulin. This finding highlights biological distinction between TP53 null phenotype mechanisms and missense TP53 mutations and encourages a

Molecular Pharmacology Fast Forward. Published on May 24, 2021 as DOI: 10.1124/molpharm.121.000254
This article has not been copyedited and formatted. The final version may differ from this version.

retrospective analysis of TP53 mutation status in available specimens from previous clinical investigations of eribulin in lung cancer patients.

Molecular Pharmacology Fast Forward. Published on May 24, 2021 as DOI: 10.1124/molpharm.121.000254
This article has not been copyedited and formatted. The final version may differ from this version.

MATERIALS AND METHODS

Cell Culture. All cell lines were cultured in RPMI-1640 growth medium supplemented with 5% fetal bovine serum at 37°C in an humidified 5% CO2 incubator. The cell lines were available in our laboratory or obtained directly from the University of Colorado Cancer Center Cell Technology shared resource and were cultured less than 6 months after receipt. The shared resource routinely performs STR analyses on all banked cell lines to ensure their authenticity.

Immunoblot Analysis. For immunoblot analysis of proteins, cells were collected in phosphate-buffered saline, centrifuged (3min at 3000x rpm) and suspended in lysis buffer. Aliquots of the cell lysates containing 50 µg of protein were submitted to SDS-PAGE and immunoblotted for TP53 (#2524), MDM2 (#86934), PARP1 (#9542) and β-actin (#4967) as a loading control. All antibodies were purchased from Cell Signaling Technology (Danvers, MA).

Cell Proliferation Assay. Cell lines were plated at 100 cells per well in 96-well tissue culture plates and treated in triplicate with a range of eribulin and paclitaxel concentrations. Cell number per well was determined after 10 days of culture using a CyQUANT Direct Cell Proliferation Assay (Life Technologies, Carlsbad, CA) according to the manufacturer's instructions.

Gene Expression and Mutation Status. Baseline RNAseq for 41 of the lung cancer cell lines was obtained from the Cancer Cell Line Encyclopedia (CCLE; https://portals.broadinstitute.org/ccle). Colo699, H125 and NE18 cell lines were not analyzed in the most recently deposited CCLE RNAseq data. To include these cell lines in the overall RNA expression analysis, in-house and legacy AffyMetrix genechip datasets (CCLE) that analyzed these three cell lines as well as H2122, H358, H520, HCC44, HCC4006, H2009, HCC78, H1650, H441, H1975, A549, H460 and Calu3 were used to generate a "standard curve" for interpolating predicted RNAseq values for TP53, CDKN2A, ABCB1, CDH1 and VIM in Colo699, H125 and NE-18 cells. Somatic

Molecular Pharmacology Fast Forward. Published on May 24, 2021 as DOI: 10.1124/molpharm.121.000254
This article has not been copyedited and formatted. The final version may differ from this version.

mutation status of the lung cancer cell lines was extracted from the CCLE except for H125 (Phelps, 1996) and NE18 (Cosmic; https://cancer.sanger.ac.uk/cosmic).

Statistics. The Inhibitory Concentration $_{50}$ (IC_{50}) values were calculated with Prism 9 (GraphPad Software, San Diego, CA). The raw CyQUANT measurements (technical triplicates) were normalized to the DMSO control value (zero drug) and the $\log_{10}$ of the inhibitor concentrations were submitted to nonlinear fitting with the “log(inhibitor) vs. normalized response” analysis feature within the Prism software program to calculate IC_{50} values. The top and bottom values were not fixed in the analysis. Tabulated and graphed IC_{50} values represent the averages of two to four independent dose-response experiments, each analyzed separately. Spearman correlation was used to evaluate the association between the eribulin IC_{50} values and gene expression levels in the 44 lung cancer cell lines. The nonparametric Kruskal-Wallis method with Holm-Šídák's multiple comparison and adjusted p values was used to test for differences between groups. Statistical significance of the distribution of oncogene and tumor suppressor mutations across eribulin IC_{50} quartiles was assessed with Fisher’s exact test and the p value and odd’s ratio were calculated with Prism.

Molecular Pharmacology Fast Forward. Published on May 24, 2021 as DOI: 10.1124/molpharm.121.000254
This article has not been copyedited and formatted. The final version may differ from this version.

RESULTS

Lung cancer cell lines exhibit a broad range of sensitivity to eribulin that is not associated with histology, epithelial-mesenchymal phenotype or oncogene driver status. Human lung cancer cell lines (n=44) representing the major histological subsets and bearing diverse oncogene drivers were submitted to clonogenic growth assays in a 96-well format to test sensitivity to eribulin at concentrations ranging from 0.01 to 30 nM. Figure 1A shows dose-response curves for 12 representative cell lines including those that were the most and least sensitive to eribulin. Using dose-response data, IC_{50} values were calculated and graphed for the 44 cell lines (see Figure 1B and Table 1). The findings reveal a very wide range of eribulin IC_{50} values that was not normally distributed among the 44 cell lines (mean = 3.6 nM, SD = 14.1 nM, median = 0.25 nM) with a 17,800-fold difference between the IC_{50} values for the most (EBC-1, 0.005 nM) and least (H1155, 88.6 nM) sensitive cell line. A subset of the lung cancer cell lines (n=32) that did not include the most eribulin-resistant cell lines was tested for sensitivity to the taxane-based microtubule inhibitor, paclitaxel. As shown in Figure 1C, the range of the paclitaxel IC_{50} values was less broad (8.8-fold) than that exhibited by eribulin (173-fold) in the same panel of 32 cell lines. Notably, regression analysis of plotted IC_{50} values for eribulin versus paclitaxel amongst the 32 cell lines (Fig. 1C) revealed a slope that was not different than zero (p=0.778). The data suggest that eribulin and paclitaxel may exhibit distinct mechanisms of action in a diverse panel of lung cancer cell lines and is consistent with their distinct mechanisms of action on microtubule dynamics (Hardin et al., 2017; Swami et al., 2017).

The histology of the tumors from which the lung cancer cell lines were derived is shown in Figure 1B and Table 1 and reveals that the broad range of eribulin sensitivity is not associated with particular histological subsets of lung cancer. Moreover, as shown in Figure 2A, no statistically significant association of eribulin IC_{50} with the cell line histology was observed. E-cadherin (CDH1) and vimentin (VIM) are markers of the epithelial and mesenchymal states, respectively, and have been associated with responsiveness to eribulin in breast cancer cell

Molecular Pharmacology Fast Forward. Published on May 24, 2021 as DOI: 10.1124/molpharm.121.000254
This article has not been copyedited and formatted. The final version may differ from this version.

lines (Dezso et al., 2014). Expression (from CCLE) of CDH1 and VIM mRNA levels plotted relative to the eribulin IC_{50} values (Fig. 2B and C) reveals no statistically significant association by Spearman correlation of CDH1 (R = -0.067, P=0.665) or VIM (R = -0.148, P=0.337) with ranked eribulin sensitivity. Finally, the ratio of CDH1 to VIM expression was not associated with the eribulin IC_{50} values (R = 0.058, P = 0.708).

Precision oncology in lung cancer is predicated on the observed vulnerability of oncogene-targeted agents in subsets of patients whose tumors bear associated mutations. The frequency of defined lung cancer oncogene drivers in cell lines was correlated with the 1st versus the 2nd-4th eribulin IC_{50} quartiles as assessed by Fisher's exact test (Table 2). As shown in Figure 1B and Table 2, lung cancer cell lines bearing oncogenic KRAS mutations (n=20) were equally distributed among the eribulin sensitivity quartiles. Due to the low number of lung cancer cell lines individually bearing oncogenic EGFR, ALK or ROS1 (7 total), these mutations were considered as a group. There was no statistically significant enrichment of lung cancer cell lines bearing mutated or rearranged receptor tyrosine kinases (EGFR, ALK, ROS1) in the most sensitive quartile of lung cancer cell lines. We previously reported that lung cancer cell lines in which FGFR1 is amplified or overexpressed exhibit increased growth dependence on this receptor tyrosine kinase (Wynes et al., 2014). The 6 cell lines previously demonstrated to overexpress FGFR1 and exhibit growth dependence were not enriched either positively or negatively in the most eribulin sensitive quartile (Table 2). Finally, similar analysis of the distribution of the 4 lines bearing mutated PIK3CA revealed a lack of statistical association, although the number of cell lines bearing this oncogene was not sufficient for rigorous assessment. The findings indicate that the eribulin sensitivity inherent in the 1st quartile of lung cancer cell lines is not associated with defined oncogene drivers.

Selected lung cancer cell lines that represent the broad range of eribulin sensitivity shown in Figure 1 were treated for 1 to 3 days with an IC_{50} dose of eribulin or DMSO as a control and cell extracts were submitted to immunoblot analysis for PARP1 (Fig. 3). The results

Molecular Pharmacology Fast Forward. Published on May 24, 2021 as DOI: 10.1124/molpharm.121.000254
This article has not been copyedited and formatted. The final version may differ from this version.

reveal that eribulin treatment induced PARP cleavage, a biochemical measure associated with apoptosis in SW900, H1581, H3122 and H460 cells, but not in Calu6, H1373, H2122 or Colo699 cells. Thus, the potency of growth inhibition by eribulin among these 8 cell lines is not associated with induction of PARP cleavage.

Eribulin sensitivity associates with TP53 mRNA expression and mutation status. TP53 mRNA levels assessed by RNAseq were extracted from the CCLE and plotted with the ranked eribulin IC_{50} values in Figure 4A. The Spearman correlation coefficient and P value were 0.466 and 0.001, respectively, indicating a highly significant association with eribulin sensitivity. When TP53 mRNA levels were assessed amongst the eribulin IC_{50} quartiles, the mRNA levels in the 1st quartile were significantly lower than the 2nd-4th quartiles (Fig. 4B). When the 44 lung cancer cell lines were classified as TP53 null (nonsense/frameshift mutations, homozygous deletion (H358)) versus TP53 wild-type and missense mutations, the 1st quartile of eribulin-sensitive cell lines was highly enriched for TP53 null alleles (Table 2, Fisher's exact test $p<0.0001$, odds ratio = 25.2). Segregation of the cell lines and associated eribulin IC_{50} values into TP53 wild-type, TP53 null alleles and TP53 missense mutations again demonstrates increased sensitivity of the TP53 null subset relative to groups bearing TP53 wild-type or missense mutations (Fig. 4C). By contrast, analysis of the association of eribulin sensitivity (1st quartile vs. 2nd-4th quartiles) and the mutation status of the tumor suppressor genes, CDKN2A ($p>0.99$), STK11/LKB1 ($p=0.41$) and KEAP1 ($p=0.24$), by Fisher's exact test did not reveal statistically significant associations (Table 2).

Within the 1st quartile of eribulin IC_{50} values, H2122 and H3122 cells express abundant mRNA levels of TP53 bearing missense mutations (Fig. 4A) and are, thus, exceptions to the null TP53 status. Immunoblot analysis of cell extracts from selected cell lines within the 1st and 2nd eribulin IC_{50} quartiles verified basal TP53 protein expression in H2122, H3122, RERF-LC-Ad2 and SW1573 cells (Fig. 5). Notably, inspection of RNAseq data from the CCLE indicated levels

Molecular Pharmacology Fast Forward. Published on May 24, 2021 as DOI: 10.1124/molpharm.121.000254
This article has not been copyedited and formatted. The final version may differ from this version.

of MDM2 mRNA greater than the mean expression value (10.5 + 7.2 FPKM) in H2122, H3122 and SW1573 cells (Table 1). MDM2 functions as an E3 ligase targeting TP53 for destruction as well as inhibiting transcriptional function via direct protein interaction (Konopleva et al., 2020; Oliner et al., 2016). Immunoblot analysis demonstrated MDM2 protein over-expression in H2122, H3122 and SW1573 cells (Fig. 5). To explore the functionality of TP53 and MDM2 expressed in H2122, H3122 and SW1573 cells, the Cancer Dependency Map (DepMap; https://depmap.org/portal/) which archives data from genome-wide CRISPR screens of cancer cell lines was interrogated. H2122 bearing TP53 missense mutations as well as SW1573 and H460 that express wild-type TP53 exhibited markedly positive and negative dependency scores, respectively, for TP53 and MDM2. These findings are consistent with functional TP53 tumor suppressive activity in these cell lines that is counteracted by elevated MDM2. Despite TP53 and MDM2 protein and mRNA expression, eribulin-sensitive H3122 cells exhibit dependencies for TP53 and MDM2 that are similar to that observed in TP53-null Calu6, H1581 and H520 cells. Thus, these analyses indicate that a TP53 null phenotype mediated by nonsense mutations or wild-type/missense levels coincident with high MDM2 expression is associated with enhanced sensitivity to eribulin relative to lung cancer cell lines bearing TP53 missense mutations which exhibit oncogenic function (Oren and Rotter, 2010; Yue et al., 2017) or wild-type TP53 without elevated MDM2 levels. This is a potentially important finding, not only as a putative biomarker for eribulin efficacy, but also regarding insight into the mechanism of action of the drug as an anti-cancer agent.

The most eribulin-insensitive lung cancer cell lines express high levels of ABCB1 mRNA. The cell lines within the 4th quartile of eribulin IC_{50} values were investigated for possible mechanisms accounting for their relative insensitivity. Using RNAseq data available from the CCLE, we performed an unbiased association of the eribulin IC_{50} values and gene expression. A positive association (Spearman R=0.436, p=0.003) with the mRNA expression of the drug

Molecular Pharmacology Fast Forward. Published on May 24, 2021 as DOI: 10.1124/molpharm.121.000254
This article has not been copyedited and formatted. The final version may differ from this version.

pump, ABCB1 (MDR1), was noted (Fig. 6A). Analysis of ABCB1 mRNA expression in the eribulin IC_{50} quartiles demonstrated that ABCB1 expression was significantly elevated in the 4th quartile relative to quartiles 1-3. This finding is consistent with the literature reporting ABCB1 as a resistance mechanism for eribulin and paclitaxel (Laughney et al., 2014; Oba et al., 2016; Vaidyanathan et al., 2016) and suggests failed intracellular drug accumulation as a likely mechanism of intrinsic resistance in this subset of the lung cancer cell lines.

Molecular Pharmacology Fast Forward. Published on May 24, 2021 as DOI: 10.1124/molpharm.121.000254
This article has not been copyedited and formatted. The final version may differ from this version.

DISCUSSION

The findings herein report the sensitivity to eribulin across a panel of 44 lung cancer cell lines that are representative of the disease. Notably, the ranked IC_{50} values do not associate with histology, driving oncogene status or epithelial-mesenchymal status. Instead, enrichment of TP53 nonsense mutations and alterations that cause loss of TP53 expression or function was observed in the lung cancer cell lines exhibiting the highest sensitivity to eribulin. A review of the literature indicates that the present analysis of 44 cancer cell lines represents the most comprehensive screen of eribulin sensitivity specific to lung cancer and therefore, provides sufficient statistical power to identify the association of sensitivity with a TP53 null phenotype. The anti-cancer activity of eribulin has been extensively explored in numerous preclinical studies (Hardin et al., 2017; Swami et al., 2017), although these generally involve experiments performed on a small number of selected cancer cell lines derived from diverse tumor types. As an example, the natural product, halichondrin B, from which the structure of eribulin is derived (Swami et al., 2017), was previously tested on the NCI-60 cancer cell line panel that includes 13 lung cancer cell lines (Bai et al., 1991). Of note, this study used drug concentrations yielding "total growth inhibition" to rank the cancer cell lines rather than the IC_{50} values calculated from dose-response relationships herein. Still, this approach identified a subset of 8-10 cancer cell lines that exhibited markedly increased halichondrin B sensitivity and included the H522 lung cancer line which is within the most sensitive quartile in the present study (Fig. 1B and Table 1). Helfrich et al (Helfrich et al., 2018) screened a panel of 17 SCLC cell lines for eribulin sensitivity and observed a much narrower range of IC_{50} values (~15 fold) relative to that observed by the 5 SCLC cell lines tested in this study (~171 fold), although the sensitivity range in our study is largely driven by SHP77 and DMS53 cells which highly express ABCB1 transporter mRNA and are relatively resistant to the drug (Figs. 1B and 6). Notably, inspection of the TP53 mutation status in the SCLC study did not reveal a positive association with TP53 null mutations, although no SCLC cell lines resided within the top quartile of eribulin sensitivity in the present

Molecular Pharmacology Fast Forward. Published on May 24, 2021 as DOI: 10.1124/molpharm.121.000254
This article has not been copyedited and formatted. The final version may differ from this version.

study either. Fisher's exact test analysis of our data after removal of the five SCLC cell lines does not alter the statistical significance (p=0.0003 versus p=0.0004) or the odds ratio (20.2 versus 20.7). In this regard, it is possible that the association of eribulin sensitivity with a null TP53 mutation status in lung cancer cell lines may be restricted to a cellular context inherent in LUAD and LUSC, but not SCLC. In addition, it would be of interest to determine if the eribulin sensitization of TP53 null lung cancer cell lines is observed in cancer cell lines derived from other cancer types, especially breast cancer where the drug is an approved agent in the therapeutic arsenal.

TP53 is a transcription factor that serves as a key cell stress-induced regulator of anti-cancer defense pathways and is the most frequently mutated oncoprotein in human neoplasms (Donehower et al., 2019; Goldstein et al., 2011; Olivier et al., 2010; Oren and Rotter, 2010). Somatic TP53 alterations observed in cancers can be classified as truncating mutations (nonsense, frameshift deletions or insertions, splice sites) or missense mutations (single nucleotide variations, in-frame deletions or insertions) where the latter are enriched within regions of the gene encoding the DNA binding domain. While truncating mutations generally lead to loss of TP53 mRNA expression due to nonsense-mediated mRNA decay processes (Donehower et al., 2019), debate continues regarding the activities intrinsic to TP53 proteins bearing missense mutations relative to wild-type TP53 (Donehower et al., 2019; Goldstein et al., 2011; Olivier et al., 2010; Oren and Rotter, 2010). Evidence indicates that, in addition to abrogating tumor suppressor activities of wild-type TP53, missense mutations also provide a gain of function that contribute to the transformed phenotype of cancer cells. The central observation in the present study that the highest eribulin sensitivity is observed in lung cancer cell lines specifically bearing a TP53 null status due to nonsense, frameshift and splice site mutations has not been previously reported. In fact, there appears to be little or no precedent for therapeutic vulnerability associated with a null TP53 status relative to a missense or wild-type TP53 mutation status. As a class, microtubule targeting agents impair microtubule dynamics

Molecular Pharmacology Fast Forward. Published on May 24, 2021 as DOI: 10.1124/molpharm.121.000254
This article has not been copyedited and formatted. The final version may differ from this version.

required for mitosis (Hardin et al., 2017). The association of a TP53 null mutation status with sensitivity to eribulin, an inhibitor of microtubule polymerization that induces sequestration of tubulin into nonfunctional aggregates, was not observed with paclitaxel which promotes tubulin polymerization and microtubule stabilization (Hardin et al., 2017; Swami et al., 2017). Based on the distinct molecular mechanisms of these microtubule targeting agents, the present findings support an hypothesis that nonfunctional tubulin aggregation induced by eribulin treatment represents a molecular signal that can discriminate a complete loss of TP53 function from the functions inherent in wild-type TP53 as well as TP53 proteins bearing missense mutations. Thus, eribulin may provide a therapeutic approach to targeting cancers presenting with a null TP53 status that can be identified by nonsense mutations detected by genomic sequencing, low mRNA or protein levels or elevated MDM2 levels such as in H2122 cells. These approaches could complement the use of MDM2 inhibitors in tumors bearing wild-type TP53 with elevated MDM2 activity and emerging compounds that allow TP53 missense mutant proteins to regain wild-type activities (Duffy et al., 2020).

Eribulin yields modest response rates in unselected, pretreated lung cancer patients (Gitlitz et al., 2012; Katakami et al., 2017; Spira et al., 2012; Swami et al., 2017). The results of this study support a retrospective analysis of TP53 mutations in available lung tumor tissues from completed eribulin trials. Alternatively, eribulin responsiveness could be assessed in lung cancer patients for which molecular-level mutation testing has been performed. In this regard, precision medicine with oncogene-targeted agents including TKIs specific for EGFR, ALK and ROS1 requires routine molecular testing on biopsies obtained from lung cancer patients and could facilitate investigation of eribulin activity in TP53-defined patient subsets going forward. Inspection of LUAD and LUSC TCGA data indicates that 21 and 30% of these lung cancers bear null TP53 perturbations, respectively (http://www.cbioportal.org/). Our findings suggest that further clinical exploration of eribulin in lung cancer patients might be directed towards patients

Molecular Pharmacology Fast Forward. Published on May 24, 2021 as DOI: 10.1124/molpharm.121.000254
This article has not been copyedited and formatted. The final version may differ from this version.

whose tumors bear TP53 null mutations and not restricted to subsets defined by histological classifications or driver oncogene status.

Molecular Pharmacology Fast Forward. Published on May 24, 2021 as DOI: 10.1124/molpharm.121.000254
This article has not been copyedited and formatted. The final version may differ from this version.

ACKNOWLEDGMENTS

We acknowledge assistance from the University of Colorado Cancer Center Cell Technology shared resource for some of the lung cancer cell lines used in the studies.

AUTHOR'S CONTRIBUTIONS

Participated in research design: Hinz, Kalkur, Rabinovitch, Hinkle, Heasley

Conducted experiments: Hinz, Kalkur, Rabinovitch, Hinkle

Performed data analysis: Hinz, Kalkur, Rabinovitch, Hinkle, Heasley

Wrote or contributed to the writing of the manuscript: Heasley, Hinz,

Molecular Pharmacology Fast Forward. Published on May 24, 2021 as DOI: 10.1124/molpharm.121.000254
This article has not been copyedited and formatted. The final version may differ from this version.

REFERENCES

Bai RL, Paull KD, Herald CL, Malspeis L, Pettit GR and Hamel E (1991) Halichondrin B and homohalichondrin B, marine natural products binding in the vinca domain of tubulin. Discovery of tubulin-based mechanism of action by analysis of differential cytotoxicity data. *The Journal of biological chemistry* **266**(24): 15882-15889.

Camidge DR, Doebele RC and Kerr KM (2019) Comparing and contrasting predictive biomarkers for immunotherapy and targeted therapy of NSCLC. *Nat Rev Clin Oncol* **16**(6): 341-355.

Dezso Z, Oestreicher J, Weaver A, Santiago S, Agoulnik S, Chow J, Oda Y and Funahashi Y (2014) Gene expression profiling reveals epithelial mesenchymal transition (EMT) genes can selectively differentiate eribulin sensitive breast cancer cells. *PloS one* **9**(8): e106131.

Donehower LA, Soussi T, Korkut A, Liu Y, Schultz A, Cardenas M, Li X, Babur O, Hsu TK, Lichtarge O, Weinstein JN, Akbani R and Wheeler DA (2019) Integrated Analysis of TP53 Gene and Pathway Alterations in The Cancer Genome Atlas. *Cell reports* **28**(11): 3010.

Duffy MJ, Synnott NC, O'Grady S and Crown J (2020) Targeting p53 for the treatment of cancer. *Semin Cancer Biol*.

Gitlitz BJ, Tsao-Wei DD, Groshen S, Davies A, Koczywas M, Belani CP, Argiris A, Ramalingam S, Vokes EE, Edelman M, Hoffman P, Ballas MS, Liu SV and Gandara DR (2012) A phase II study of halichondrin B analog eribulin mesylate (E7389) in patients with advanced non-small cell lung cancer previously treated with a taxane: a California cancer consortium trial. *J Thorac Oncol* **7**(3): 574-578.

Goldstein I, Marcel V, Olivier M, Oren M, Rotter V and Hainaut P (2011) Understanding wild-type and mutant p53 activities in human cancer: new landmarks on the way to targeted therapies. *Cancer Gene Ther* **18**(1): 2-11.

Hardin C, Shum E, Singh AP, Perez-Soler R and Cheng H (2017) Emerging treatment using tubulin inhibitors in advanced non-small cell lung cancer. *Expert Opin Pharmacother* **18**(7): 701-716.

Helfrich BA, Gao D and Bunn PA, Jr. (2018) Eribulin inhibits the growth of small cell lung cancer cell lines alone and with radiotherapy. *Lung Cancer* **118**: 148-154.

Katakami N, Felip E, Spigel DR, Kim JH, Olivo M, Guo M, Nokihara H, Yang JC, Iannotti N, Satouchi M and Barlesi F (2017) A randomized, open-label, multicenter, phase 3 study to compare the efficacy and safety of eribulin to treatment of physician's choice in patients with advanced non-small cell lung cancer. *Ann Oncol* **28**(9): 2241-2247.

Konopleva M, Martinelli G, Daver N, Papayannidis C, Wei A, Higgins B, Ott M, Mascarenhas J and Andreeff M (2020) MDM2 inhibition: an important step forward in cancer therapy. *Leukemia* **34**(11): 2858-2874.

Laughney AM, Kim E, Sprachman MM, Miller MA, Kohler RH, Yang KS, Orth JD, Mitchison TJ and Weissleder R (2014) Single-cell pharmacokinetic imaging reveals a therapeutic strategy to overcome drug resistance to the microtubule inhibitor eribulin. *Science Translational Medicine* **6**(261): 261ra152.

Mok TS, Wu YL, Thongprasert S, Yang CH, Chu DT, Saijo N, Sunpaweravong P, Han B, Margono B, Ichinose Y, Nishiwaki Y, Ohe Y, Yang JJ, Chewaskulyong B, Jiang H, Duffield EL, Watkins CL, Armour AA and Fukuoka M (2009) Gefitinib or carboplatin-paclitaxel in pulmonary adenocarcinoma. *N Engl J Med* **361**(10): 947-957.

Oba T, Izumi H and Ito KI (2016) ABCB1 and ABCC11 confer resistance to eribulin in breast cancer cell lines. *Oncotarget* **7**(43): 70011-70027.

Oliner JD, Saiki AY and Caenepeel S (2016) The Role of MDM2 Amplification and Overexpression in Tumorigenesis. *Cold Spring Harbor perspectives in medicine* **6**(6): a026336.

Olivier M, Hollstein M and Hainaut P (2010) TP53 mutations in human cancers: origins, consequences, and clinical use. *Cold Spring Harb Perspect Biol* **2**(1): a001008.

Oren M and Rotter V (2010) Mutant p53 gain-of-function in cancer. *Cold Spring Harb Perspect Biol* **2**(2): a001107.

Pacheco JM, Camidge DR, Doebele RC and Schenk E (2019) A Changing of the Guard: Immune Checkpoint Inhibitors With and Without Chemotherapy as First Line Treatment for Metastatic Non-small Cell Lung Cancer. *Front Oncol* **9**: 195.

Phelps RM, Johnson, B.E., Ihde, D.C. Gazdar, A.F., Carbone, D.P., McClintock, P.R., Linnoila, R.I., Matthews, M.J., Bunn, P.A., Jr., Carney, D., Minna, J.D., and Mulshine, J.L. (1996) NCI-Navy medical oncology branch cell line data base. *J Cellular Biochemistry Supplement* **24**: 32-91.

Politi K and Herbst RS (2015) Lung cancer in the era of precision medicine. *Clin Cancer Res* **21**(10): 2213-2220.

Shepherd FA, Rodrigues Pereira J, Ciuleanu T, Tan EH, Hirsh V, Thongprasert S, Campos D, Maoleekoonpiroj S, Smylie M, Martins R, van Kooten M, Dediu M, Findlay B, Tu D, Johnston D, Bezjak A, Clark G, Santabarbara P and Seymour L (2005) Erlotinib in previously treated non-small-cell lung cancer. *N Engl J Med* **353**(2): 123-132.

Spira AI, Iannotti NO, Savin MA, Neubauer M, Gabrail NY, Yanagihara RH, Zang EA, Cole PE, Shuster D and Das A (2012) A phase II study of eribulin mesylate (E7389) in patients with advanced, previously treated non-small-cell lung cancer. *Clin Lung Cancer* **13**(1): 31-38.

Swami U, Shah U and Goel S (2017) Eribulin in non-small cell lung cancer: challenges and potential strategies. *Expert Opin Investig Drugs* **26**(4): 495-508.

Thatcher N, Chang A, Parikh P, Rodrigues Pereira J, Ciuleanu T, von Pawel J, Thongprasert S, Tan EH, Pemberton K, Archer V and Carroll K (2005) Gefitinib plus best supportive care in previously treated patients with refractory advanced non-small-cell lung cancer:

results from a randomised, placebo-controlled, multicentre study (Iressa Survival Evaluation in Lung Cancer). *Lancet* **366**(9496): 1527-1537.

Vaidyanathan A, Sawers L, Gannon AL, Chakravarty P, Scott AL, Bray SE, Ferguson MJ and Smith G (2016) ABCB1 (MDR1) induction defines a common resistance mechanism in paclitaxel- and olaparib-resistant ovarian cancer cells. *British journal of cancer* **115**(4): 431-441.

Wynes MW, Hinz TK, Gao D, Martini M, Marek LA, Ware KE, Edwards MG, Bohm D, Perner S, Helfrich BA, Dziadziuszko R, Jassem J, Wojtylak S, Sejda A, Gozgit JM, Bunn PA, Jr., Camidge DR, Tan AC, Hirsch FR and Heasley LE (2014) FGFR1 mRNA and protein expression, not gene copy number, predict FGFR TKI sensitivity across all lung cancer histologies. *Clin Cancer Res* **20**(12): 3299-3309.

Yue X, Zhao Y, Xu Y, Zheng M, Feng Z and Hu W (2017) Mutant p53 in Cancer: Accumulation, Gain-of-Function, and Therapy. *J Mol Biol* **429**(11): 1595-1606.

Molecular Pharmacology Fast Forward. Published on May 24, 2021 as DOI: 10.1124/molpharm.121.000254
This article has not been copyedited and formatted. The final version may differ from this version.

Footnotes

The studies were supported by a research grant to L. Heasley from Eisai Company. We also acknowledge support of the University of Colorado Cancer Center Core grant (NIH P30 CA046934) and the Cell Technology shared resource.

While Eisai Company supported this study and also developed and commercialized eribulin, an agent investigated in this report, Eisai was not involved in study design or data analysis. Thus, there is no conflict of interest regarding the studies herein.

Molecular Pharmacology Fast Forward. Published on May 24, 2021 as DOI: 10.1124/molpharm.121.000254
This article has not been copyedited and formatted. The final version may differ from this version.

FIGURE LEGENDS

Figure 1. Eribulin sensitivity of 44 lung cancer cell lines. Cells were plated at 100 cells per well in 96-well tissue culture plates and treated with eribulin at concentrations of 0 to 30 nM. After 10 days of incubation, cell numbers were estimated using a CyQUANT Direct Cell Proliferation Assay (Invitrogen) according to the manufacturer's instructions. **A,** Eribulin dose-response curves are shown for 12 representative lung cancer cell lines, including the 5 most sensitive and 5 of the least sensitive cell lines, **B,** Eribulin IC_{50} values are plotted for all 44 cell lines tested and annotated for histological subtype as indicated in the key. Note the data are plotted as log_{10} due to the broad range in sensitivities across the cell line panel. The mean $\pm$ SD IC_{50} was 3.6 nM $\pm$14.1 nM and the median value was 0.246 nM. The eribulin IC_{50} values were not normally distributed across the panel of lung cancer cell lines (D'Agostino & Pearson normality test, $p< 0.0001$). The bar graph is annotated with the dominant tumor suppressors and driving oncogene as defined in the color key. **C,** Cells were plated at 100 cells per well in 96-well tissue culture plates and treated with paclitaxel at concentrations of 0 to 30 nM . After 10 to 14 days of incubation, cell numbers were estimated using a CyQUANT Direct Cell Proliferation Assay (Invitrogen) according to the manufacturer's instructions. Eribulin IC_{50} values from Figure 1B and Table 1 are plotted for 32 cell lines along with the IC_{50} values determined for paclitaxel (note the y-axis is log_{10}). The eribulin and paclitaxel IC_{50} values for the 32 cell lines were plotted as indicated and the data submitted to linear regression analysis. The slope (0.0213) was not statistically different from zero ($p=0.778$).

Figure 2. Eribulin sensitivity is not associated with cell line histology or epithelial-mesenchymal differentiation. A, The 44 lung cancer cell lines were binned by their reported histology (adenocarcinoma, squamous cell, large cell, small cell) and their calculated eribulin IC_{50} values were graphed as scatter plots with the mean and SEM indicated. Kruskal-Wallis with Holm-Šídák's multiple comparisons revealed no statistically significant differences amongst the

Molecular Pharmacology Fast Forward. Published on May 24, 2021 as DOI: 10.1124/molpharm.121.000254
This article has not been copyedited and formatted. The final version may differ from this version.

4 histological classifications. Eribulin IC_{50} values for 44 lung cancer cell lines for which CCLE gene expression data are available are shown relative to the expression of (**B**) E-cadherin (CDH1) and (**C**) vimentin (VIM). No significant correlation of eribulin IC_{50} values with CDH1 (R = -0.067, P=0.665) or VIM (R = -0.148, P=0.337) expression was observed by Spearman correlation analysis.

Figure 3. Induction of PARP1 cleavage by eribulin. Extracts from lung cancer cell lines treated for 1 to 3 days with eribulin at the indicated concentrations (~IC_{50} doses (see Figure 1 and Table 1) or DMSO as a diluent control were submitted to SDS-PAGE and immunoblotted for PARP1 (CST #9542). The filters were stripped and re-probed for β-actin as a loading control.

Figure 4. Eribulin sensitivity associates with a null TP53 status. A, The ranked eribulin IC_{50} values for the 44 lung cancer cell lines are overlayed with their associated TP53 mRNA expression values (in RPKM). Spearman correlation analysis revealed a statistically significant association of eribulin IC_{50} and TP53 mRNA expression. **B**, The TP53 mRNA levels for the eribulin IC_{50} quartiles from the 44 lung cancer cell lines are presented with the mean and SD. The data were analyzed by Kruskal-Wallis with multiple comparisons. The TP53 mRNA expression in the 1^{st} quartile was significantly different from the 2^{nd}, 3^{rd} and 4^{th} quartiles. **C**, Eribulin IC_{50} values from the 44 lung cancer cell lines were binned for TP53 mutation status. WT indicates cell lines lacking nonsense or missense mutations and exhibiting significant mRNA expression levels from CCLE RNAseq data. Cell lines bearing TP53 nonsense/frameshift mutations or exhibiting wild-type, but low/absent TP53 mRNA are binned separately from cell lines bearing known TP53 missense mutations. Statistical analysis by Kruskal-Wallis with multiple comparisons reveals significantly lower eribulin IC_{50} values in cell lines binned by TP53 nonsense/missense mutations and low expression relative to cell lines bearing TP53 wild-type TP53 or missense mutations. Eribulin sensitivity of cell lines bearing TP53 wild-type and missense mutations was not statistically different.

Molecular Pharmacology Fast Forward. Published on May 24, 2021 as DOI: 10.1124/molpharm.121.000254
This article has not been copyedited and formatted. The final version may differ from this version.

Figure 5. TP53 and MDM2 expression in selected lung cancer cell lines. A, Lung cancer cell lines from the 1st eribulin IC_{50} quartile were submitted to immunoblot analysis for baseline expression of TP53 and MDM2 protein levels. The filters were stripped and re-probed for β-actin as a loading control. **B**, Publicly-available data from CRISPR/Cas9 Dependency Map (DepMap; https://depmap.org/portal/) project were interrogated for TP53 and MDM2 in the indicated lung cancer cell lines. The dependency scores are the output from CERES (https://depmap.org/ceres/) where lower scores indicate genes that are more likely to be dependent in a given cell line. The CRISPR/Cas9 screen values are from the CRISPR (Avana) Public 19Q2 dataset. A score of 0 is equivalent to a gene that is not essential whereas a score of -1 corresponds to the median of all common essential genes. Positive scores as shown for gRNAs targeting TP53 in H2122, SW1573 and H460 cells indicate enhanced cell survival upon deletion of TP53. The negative dependency scores associated with gRNAs targeting MDM2 indicate decreased cell survival in these cell lines.

Figure 6. High expression of ABCB1 mRNA in lung cancer cell lines exhibiting intrinsic resistance to eribulin. **A,** The ranked eribulin IC_{50} values for the 44 lung cancer cell lines are overlayed with their associated ABCB1 mRNA expression values (in RPKM). Spearman correlation analysis revealed a statistically significant association of eribulin IC_{50} and ABCB1 mRNA expression. **B**, The ABCB1 mRNA levels for the eribulin IC_{50} quartiles from the 44 lung cancer cell lines are presented with the mean and SD. The data were analyzed by Kruskal-Wallis with multiple comparisons. The ABCB1 mRNA expression in the 4th quartile was significantly different from the 1st, 2nd and 3rd quartiles.

Molecular Pharmacology Fast Forward. Published on May 24, 2021 as DOI: 10.1124/molpharm.121.000254
This article has not been copyedited and formatted. The final version may differ from this version.

Table 1

Cell Line	Histology	Eribulin IC_{50} (nM)	Oncogene Mutations	TP53 status	TP53 mRNA (rpkm)	MDM2 mRNA (rpkm)
EBC-1	Squamous	0.005	CCND1-P287L	E171*	2	5
SW900	Squamous	0.02	KRAS-G12V	Q167*	5	8
Calu6	Adeno	0.03	KRAS-Q61K	R196*	4	6
H522	Adeno	0.06	FGFR1 Positive	P191fs	1	13
H1373	Adeno	0.07	KRAS-G12C	E339*	2	5
H2122	Adeno	0.07	KRAS-G12C	C176F/Q16L	22	20
H358	Adeno	0.08	KRAS-G12C	homodel	0	6
H1581	Large Cell	0.08	FGFR1 Positive	Q144*	2	8
H3122	Adeno	0.08	EML4-ALK	E285V	28	11
H125	AdenoSquamous	0.09		N239fs	2	1
H520	Squamous	0.12	FGFR1 Positive	W146*	2	6
H2066	Mixed	0.15		V157F	63	20
RERF-LC-Ad2	Adeno	0.17	KRAS-G12V	A159V	26	10
SW1573	Squamous	0.17	KRAS-G12C; PIK3CA-K111E; CTNNB1-S33F	WT	26	22
HCC44	Adeno	0.18	KRAS-G12C	R175L/S94*	1	6
H1341	SCLC	0.19	PIK3CA-E542K	WT	27	12
H2228	Adeno	0.20	EML4-ALK	Q331*	5	7
DMS114	SCLC	0.20	FGFR1 positive	R213*	3	14
H661	Large Cell	0.20		R158L/S151I	20	11
H1355	Adeno	0.20	KRAS-G13C	E285K	17	17
H1573	Adeno	0.24	KRAS-G12A; NRAS-Q61K	R248L	14	14
HCC4006	Adeno	0.24	EGFR del19	Y205H	45	5
H2009	Adeno	0.25	KRAS-G12A	R273L	33	5
H211	SCLC	0.25		R248Q	19	19
LU65	Adeno	0.26	KRAS-G12C	E11Q	11	5
HCC78	Adeno	0.28	SLC34A2-ROS1	S241F	11	8
H1650	Adeno	0.34	EGFR del19	Ins-Frameshift	4	12
H441	Adeno	0.37	KRAS-G12V	R158L	27	7
H1975	Adeno	0.42	EGFR-L858R/T790M; PIK3CA-G118D	R273H	55	4
H838	Adeno	0.45		E62*	3	10
H226	Squamous	0.46	FGFR1 Positive	WT	40	44
A549	Adeno	0.61	KRAS-G12S	WT	19	17
PC-9	Adeno	0.62	EGFR del19	R248Q	29	5
NE-18	Squamous	0.92		WT	17	1
H727	Carcinoid	1.01	KRAS-G12V	Q165_S166insYKQ	25	8
H460	Large Cell	1.22	KRAS-Q61H; PIK3CA-E545K	WT	14	9
Calu3	Adeno	1.27		M237I	18	6
H2170	Squamous	1.48		R158G	23	13
H2030	Adeno	3.29	KRAS-G12C	G262V	25	7
Colo699	Adeno	4.81	FGFR1 Positive	R248L	26	12
H647	AdenoSquamous	4.91	KRAS-G13D	S261_splice	28	5
SHP-77	SCLC	10.23	KRAS-G12V	C176W	45	10
DMS53	SCLC	32.45		S241F/E56*	24	17
H1155	Large Cell	88.62	KRAS-Q61H; PTEN-R233*/F341V; APC-R232*	R273H/Y205F	16	9

Table 1. Dose response data (see Figure 1) were used to calculate the IC_{50} values for 44 cell lines using the Prism software program. The 44 cell lines are ranked by eribulin sensitivity and

Molecular Pharmacology Fast Forward. Published on May 24, 2021 as DOI: 10.1124/molpharm.121.000254
This article has not been copyedited and formatted. The final version may differ from this version.

categorized by histology, dominant oncogene mutations, TP53 mutation status and mRNA expression levels for TP53 and MDM2 derived from the CCLE.

Table 2
Distribution of oncogene and tumor suppressor mutations in eribulin IC_{50} quartiles

Category	P value	Odds ratio	95% CI
KRAS: WT vs mutant	>0.999	1	0.30 to 3.28
FGFR1: WT vs amp/high expression	0.16	0.28	0.046 to 1.64
EGFR/ALK/ROS1: WT vs mutant/fusion	0.66	2.22	0.24 to 20.83
TP53: null/low expression vs WT/missense	0.0001	25.2	4.15 to 153.0
CDKN2A: WT vs mutant/deletion	>0.999	0.78	0.19 to 3.17
KEAP1: WT vs mutant	0.24	4.35	0.49 to 38.68
STK11: WT vs mutant	0.41	3.2	0.35 to 2.83

Table 2. The distribution of the indicated oncogenes and tumor suppressors in the 1st quartile of eribulin IC_{50} values was compared to the 2nd, 3rd and 4th quartiles by Fisher's exact test and the resulting p values and odds ratios tabulated. Enrichment of lung cancer cell lines bearing a null TP53 phenotype (nonsense/truncating mutations and low mRNA expression) was the only marker significantly associated with the highest sensitivity to eribulin.

Molecular Pharmacology Fast Forward. Published on May 24, 2021 as DOI: 10.1124/molpharm.121.000254
This article has not been copyedited and formatted. The final version may differ from this version.

Molecular Pharmacology Fast Forward. Published on May 24, 2021 as DOI: 10.1124/molpharm.121.000254
This article has not been copyedited and formatted. The final version may differ from this version.

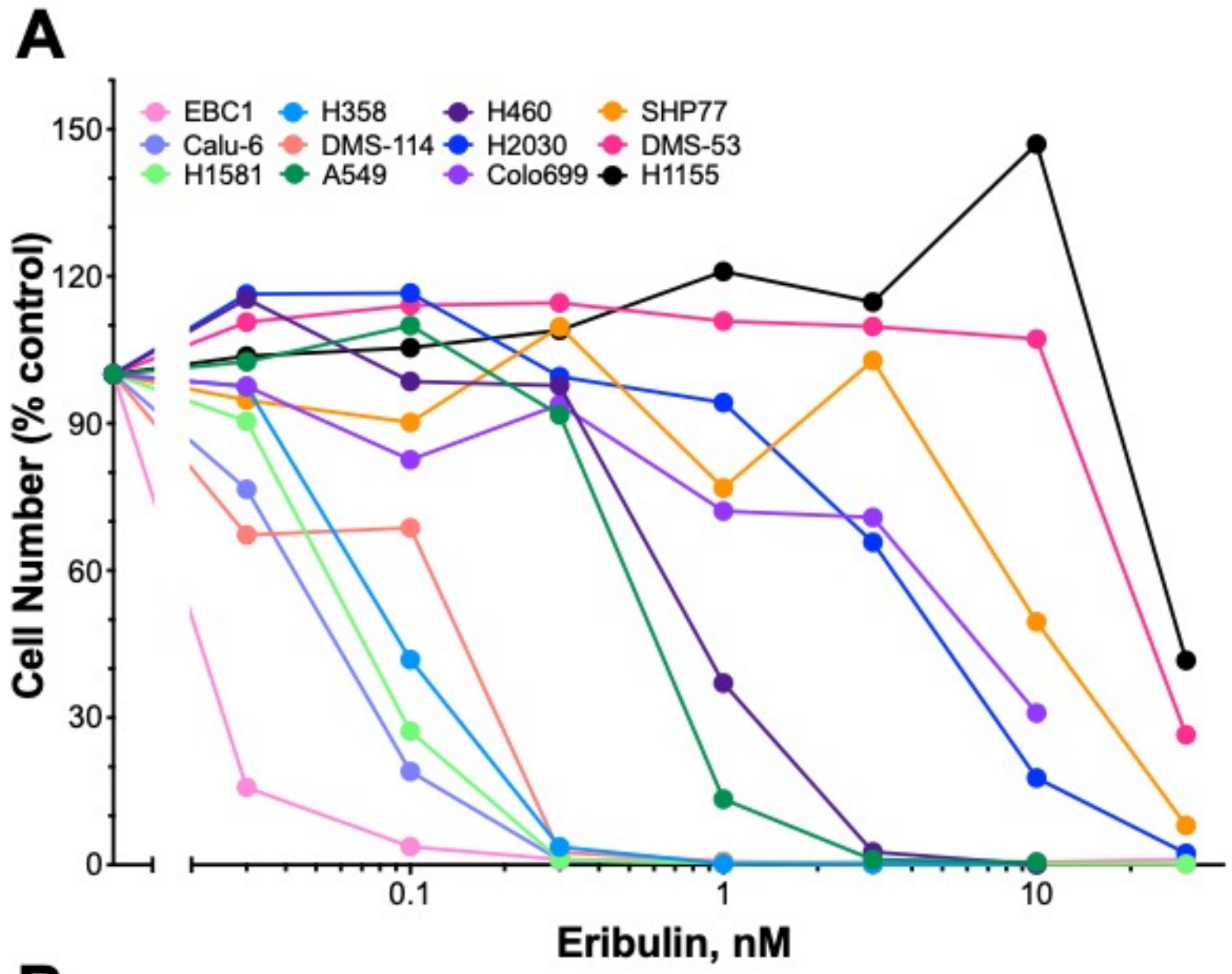

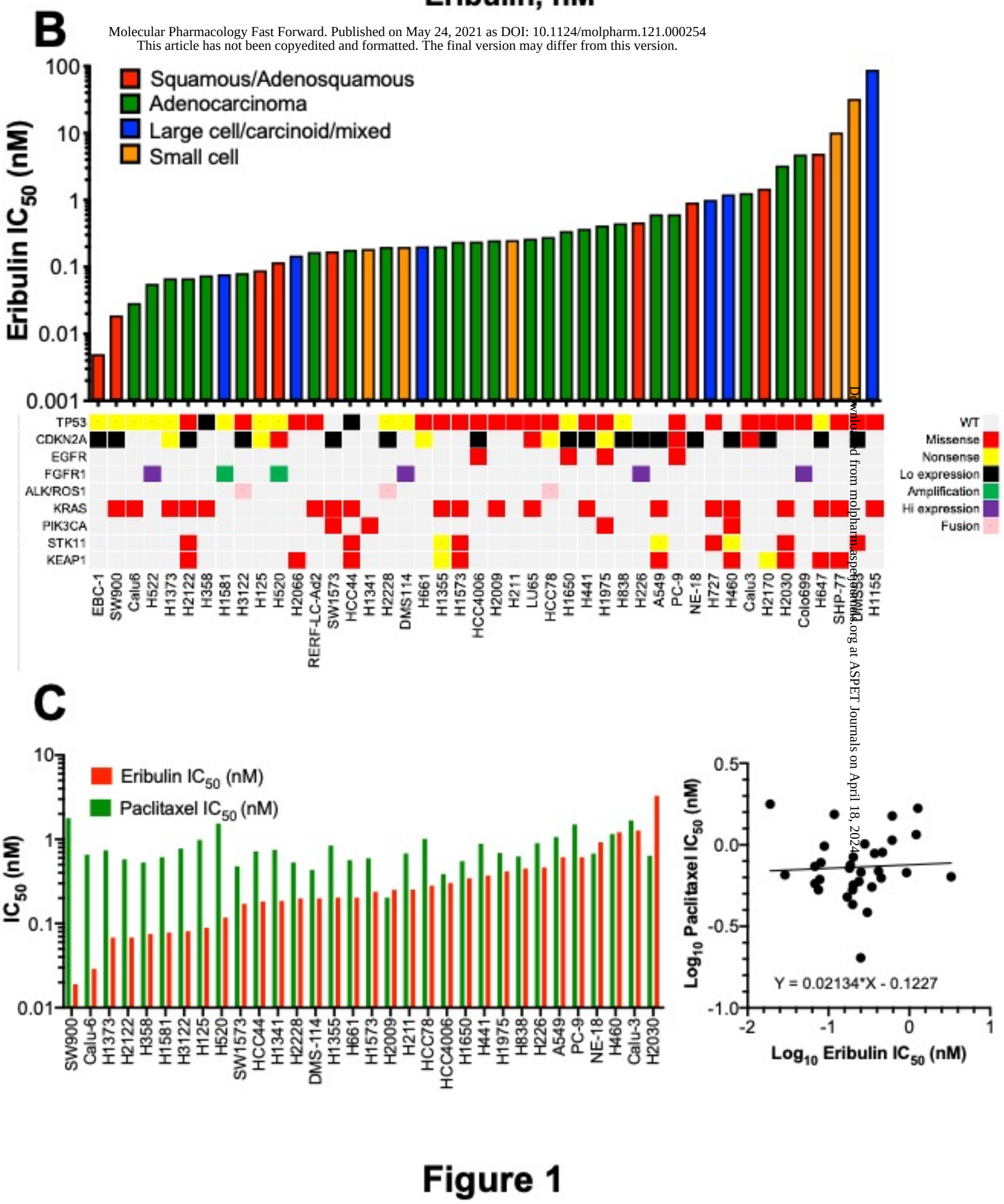

Figure 1

Molecular Pharmacology Fast Forward. Published on May 24, 2021 as DOI: 10.1124/molpharm.121.000254
This article has not been copyedited and formatted. The final version may differ from this version.

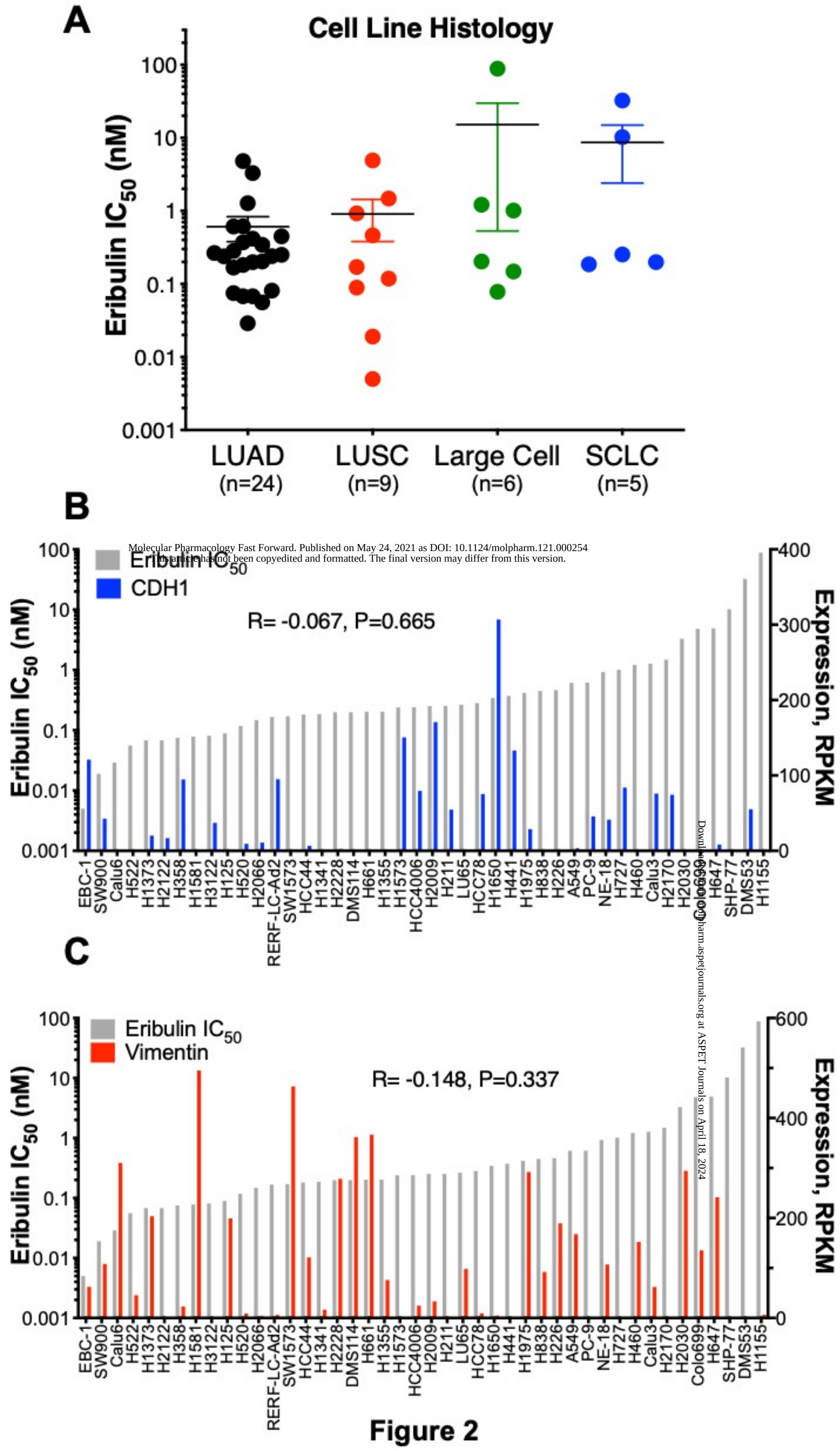

Figure 2

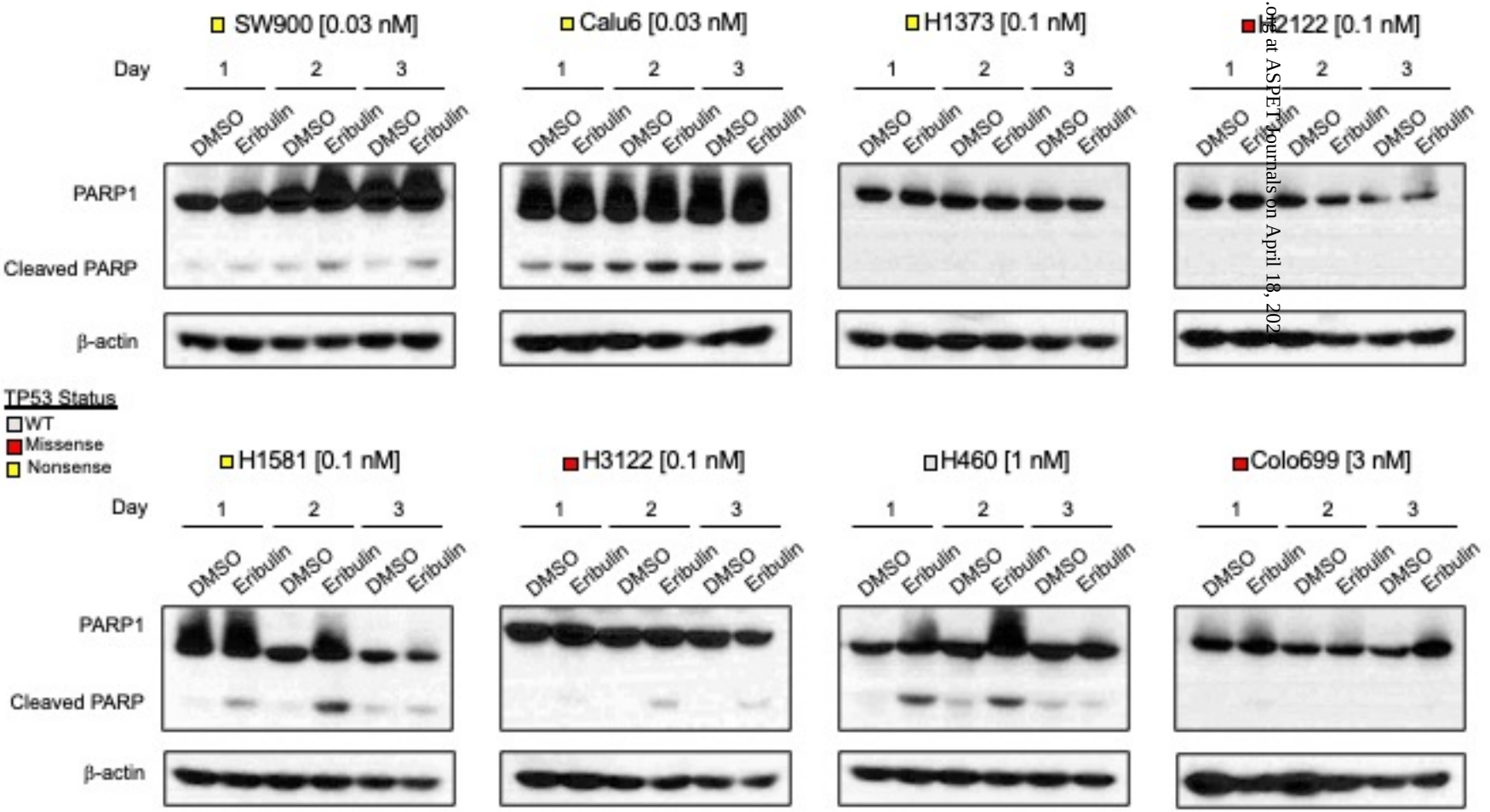

Figure 3

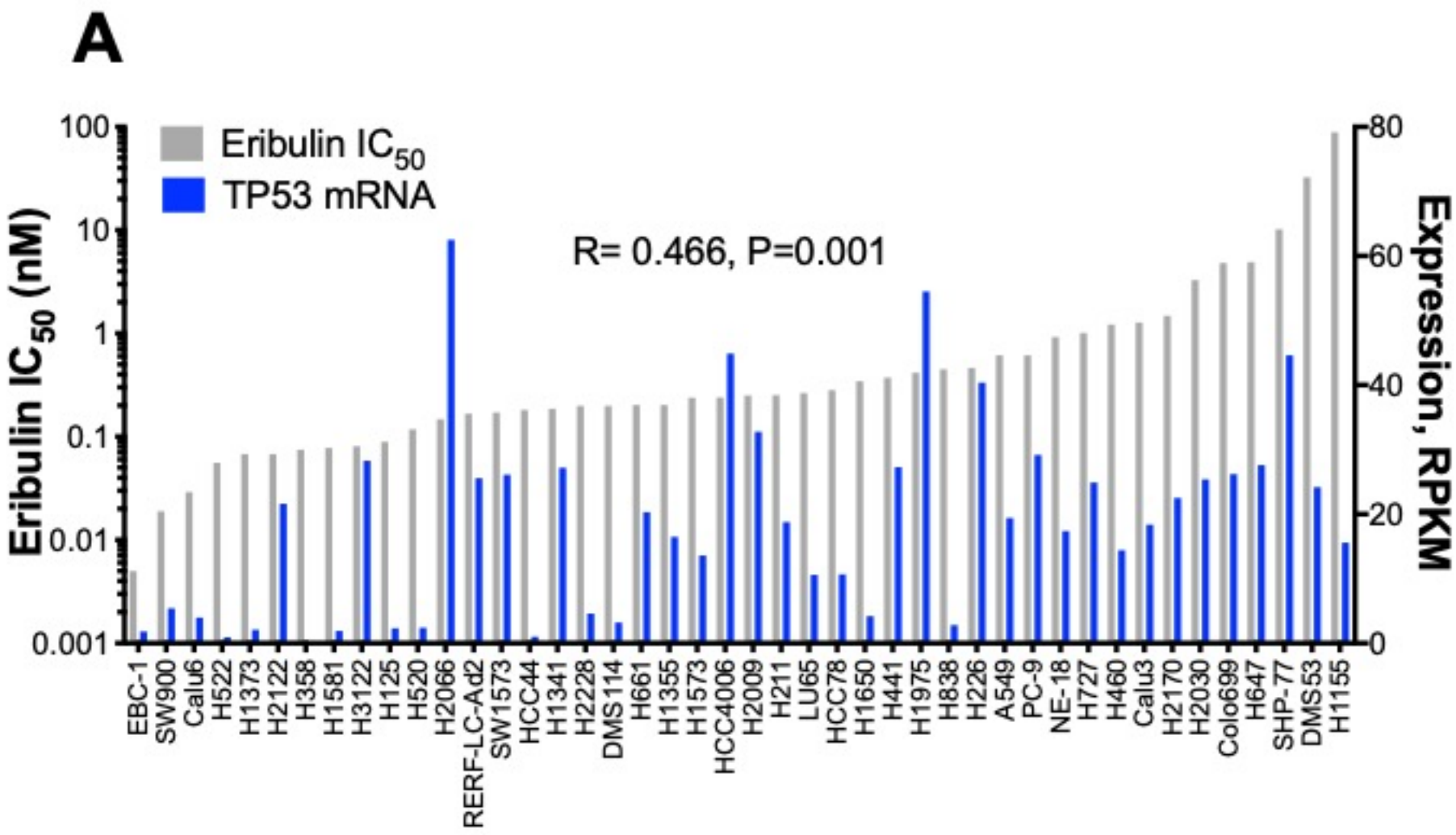

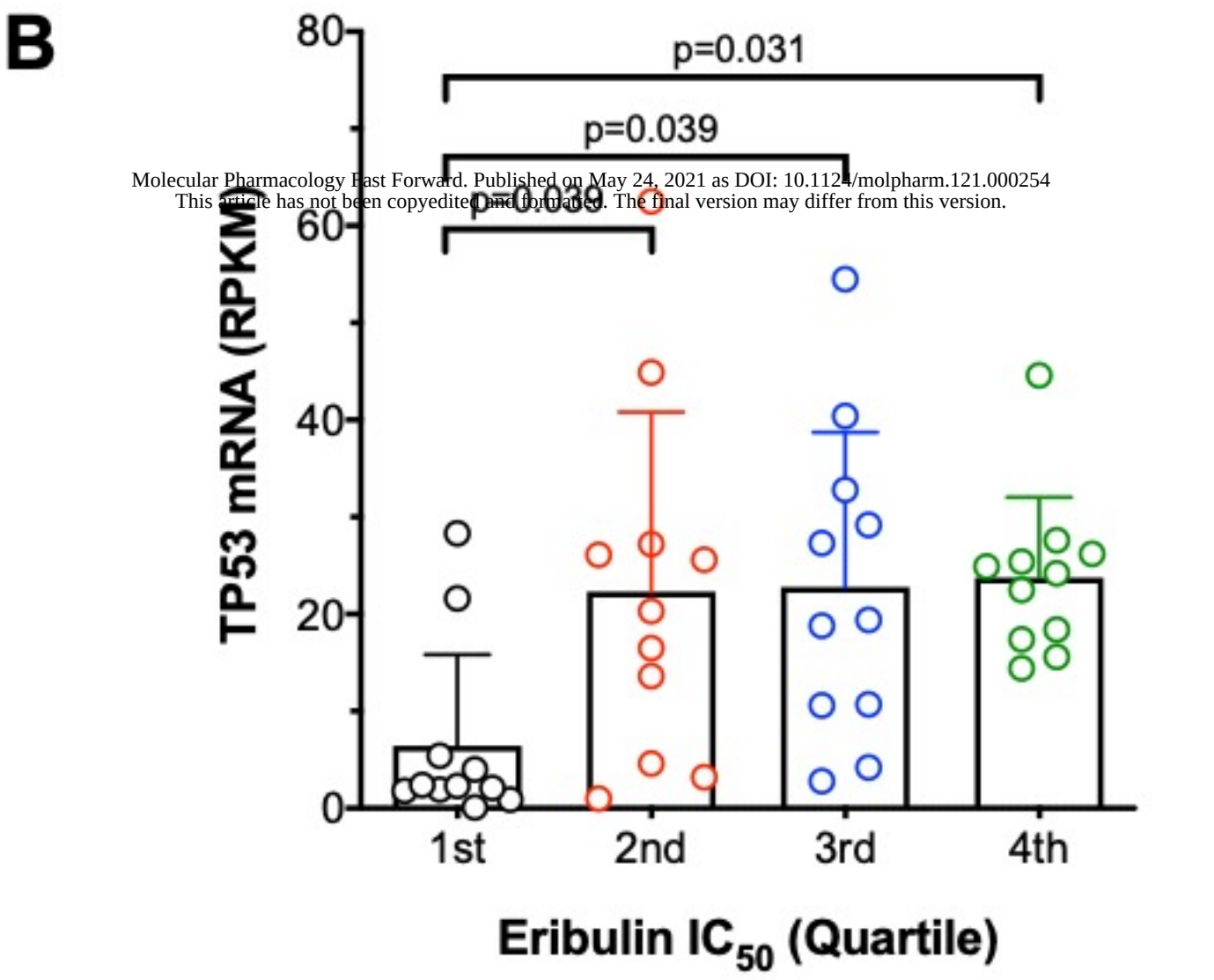

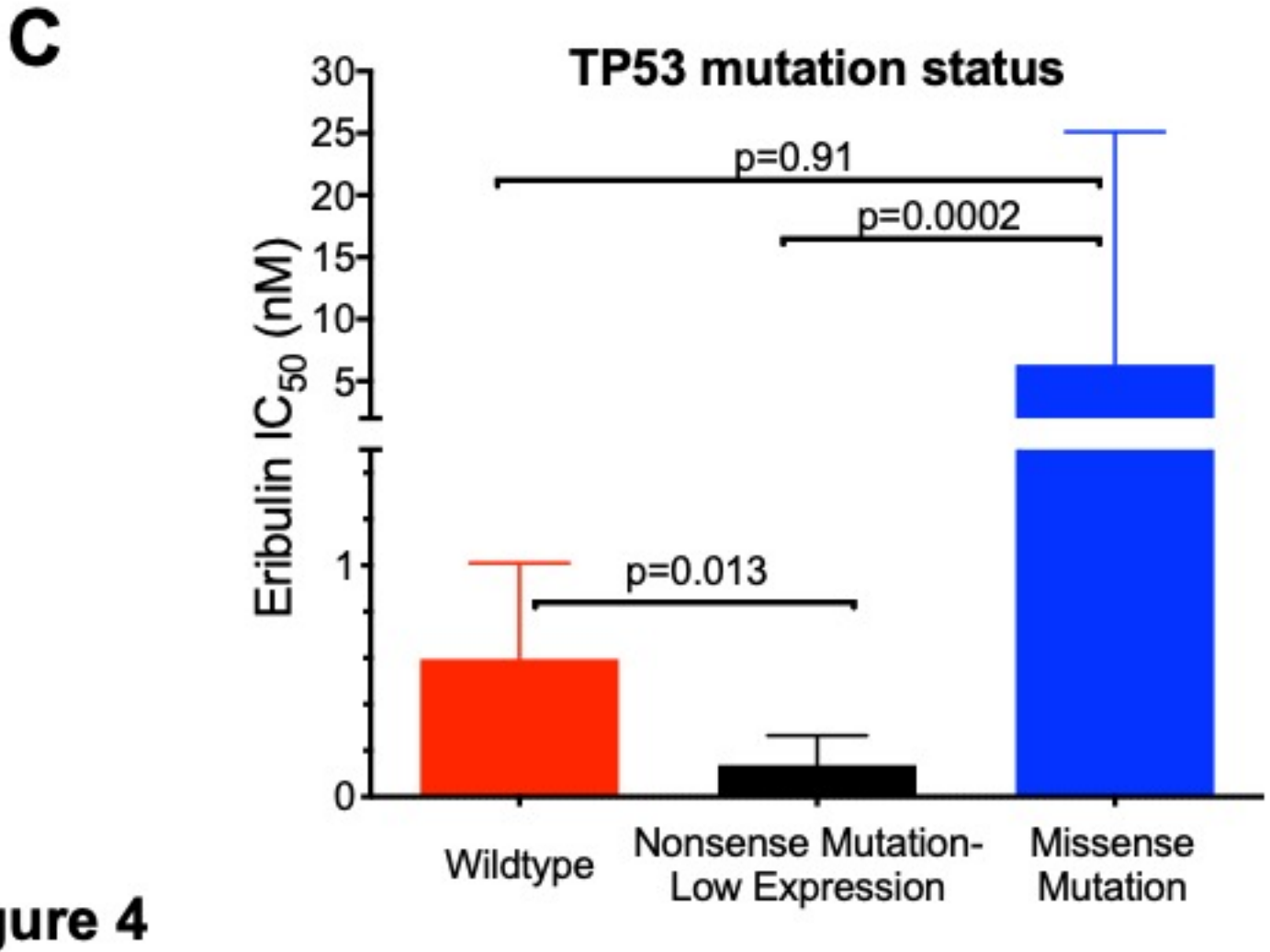

Figure 4

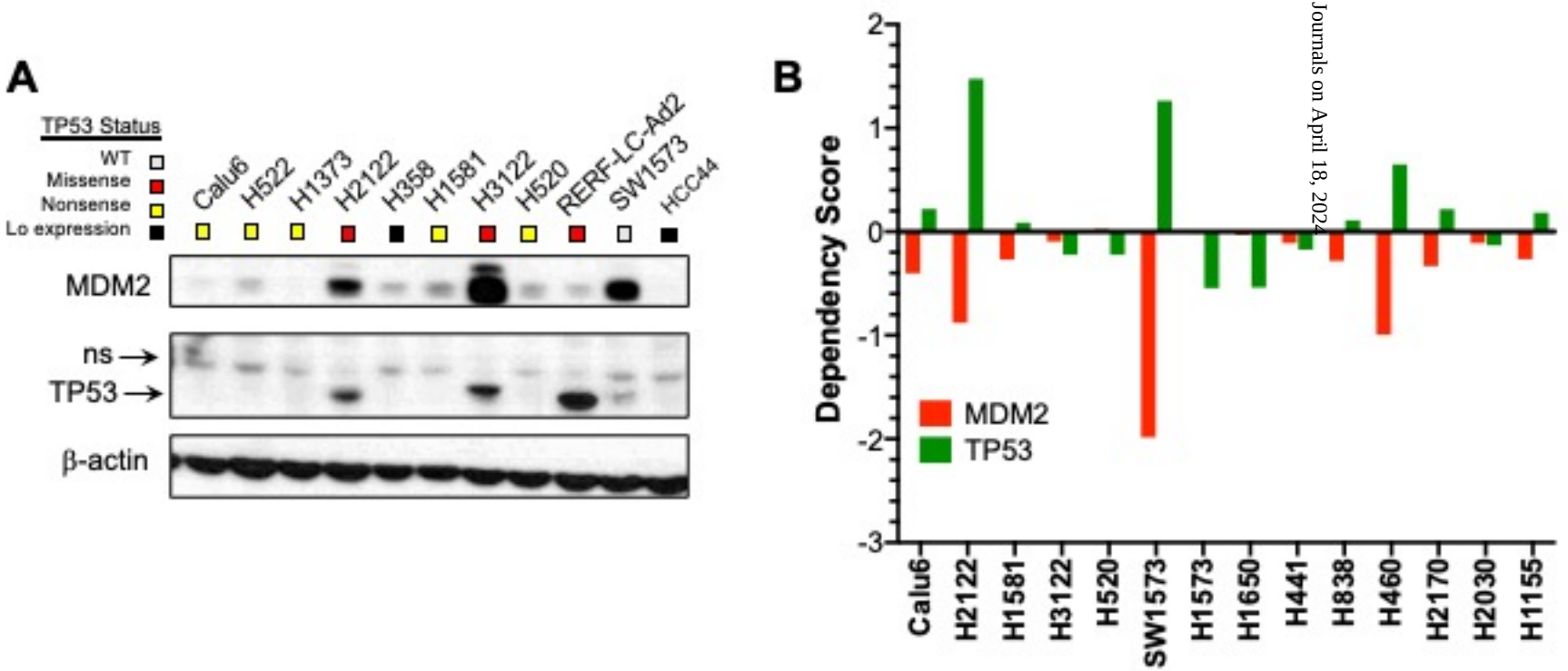

Figure 5

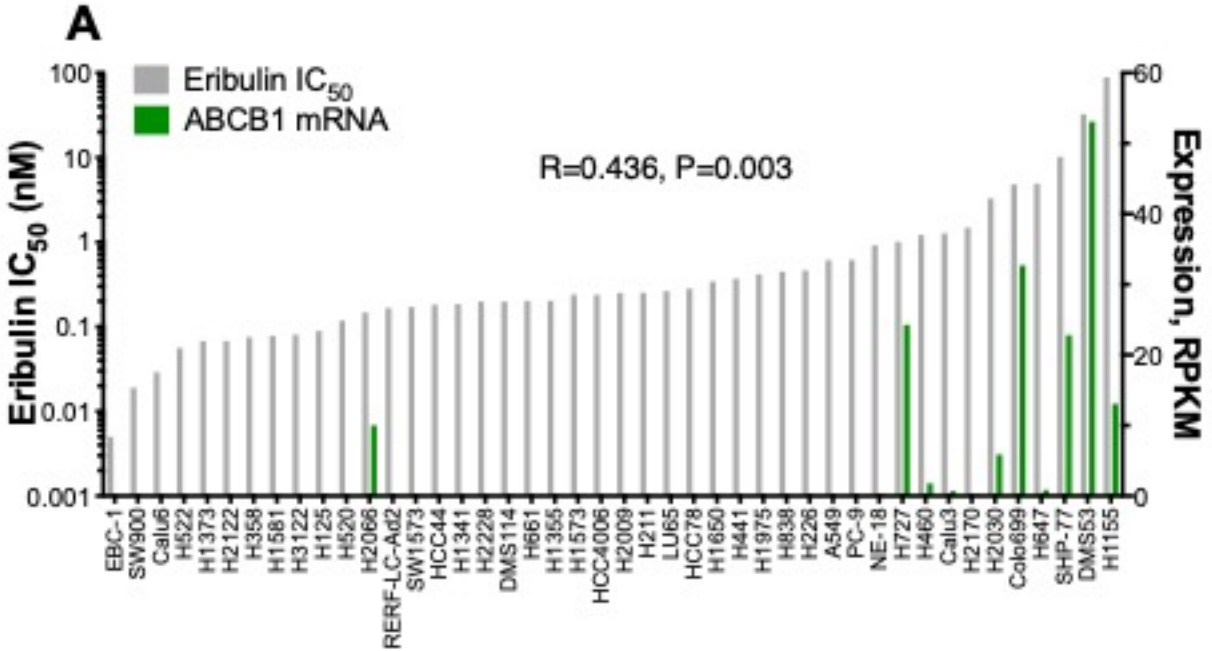

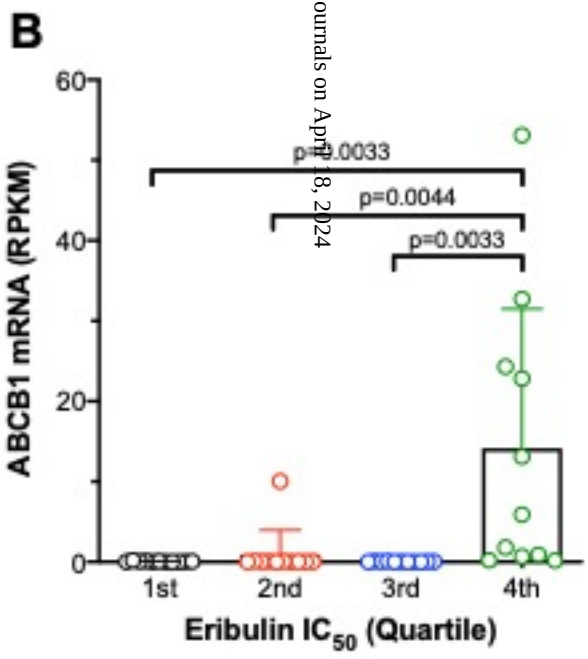

Figure 6